

# INTERNATIONAL SOCIETY FOR SOIL MECHANICS AND GEOTECHNICAL ENGINEERING



*This paper was downloaded from the Online Library of the International Society for Soil Mechanics and Geotechnical Engineering (ISSMGE). The library is available here:*

<https://www.issmge.org/publications/online-library>

*This is an open-access database that archives thousands of papers published under the Auspices of the ISSMGE and maintained by the Innovation and Development Committee of ISSMGE.*

# Short term lateral deformations induced in an elastic medium through the application of rigid embankment loading

Briony Rankine

Golder Associates, Cairns, QLD Australia

Nagaratnam Sivakugan

James Cook University, Townsville, QLD Australia

Keywords: lateral displacements, soft clays, numerical modelling, analytical solutions

## ABSTRACT

Recently, numerous investigations have been conducted to predict the lateral displacements which develop in soft clay foundations as a result of embankment construction. These studies focus on the prediction of lateral deformation at the toe of the embankment, and were prompted by observations of the damaging effects on adjacent structures by these deformations. The mechanisms of lateral deformations are not yet clearly understood, however, predictions of behaviour seem possible due to the distribution of lateral deformations with depth remaining similar during the settlement process.

The finite difference program FLAC was used within this study to model the behaviour of a homogeneous elastic medium subjected to different conditions of embankment loading. An empirical relation has been developed to describe the variation of lateral deformations with depth, at various distances from the embankment toe. This empirical correlation compared well to predictions from a previously validated numerical model of an instrumented trial embankment.

## 1 INTRODUCTION

The development of lateral deformations during and after embankment construction has been the subject of numerous studies over the years, the necessity having arisen from observations of the damage to adjacent structures including bridge abutments, piles and utilities. When soft clays are present, these lateral soil movements are particularly large, and frequently quite significant stresses can be generated (Broms, 1972; Huder and Bucher, 1981). This stress-strain behaviour conforms to the idea that when a load is applied to the soil surface, the vertical stress within the soil mass is increased and extends indefinitely in all directions. The lateral soil movements induced through the intensity of these applied loads will generate passive loadings and subsequently passive stresses on nearby structures.

Of the existing research which has been conducted in the field of deformation analysis below embankment loading, the majority focuses upon deformations in relation to the stability of the embankment and soil behaviour within the system. Poulos and Davis (1974) presented elastic solutions to account for the distribution of horizontal and vertical displacement within a foundation of finite depth. Displacements were predicted at the base of the embankment and are described using an equation. Use of this equation for lateral deformation prediction is, however, limited due to the development and consideration of limited geometries.

This paper describes the development of a series of equations useful in determining the location and magnitude of short-term lateral soil displacement. They describe the displacement profile not only at the embankment toe, but also at various distances away from it. All equations have been non-dimensionalised so that they are able to be used for a variety of soil types.

## 2 MODELLING ASSUMPTIONS AND CONSIDERATIONS

A number of theoretical assumptions were made during formulation of the equations shown subsequently within this paper. Foremost to these, was the assumption of an elastic constitutive model. The second principal assumption was that of a plane strain condition. And the third main assumption was that of a homogeneous, isotropic material in a semi-infinite half space in which the soil medium initially assumed to be bounded with a horizontal ground surface extending infinitely in both width and depth. This assumption has been applied previously by many researchers (Fadum,

1948; Osterberg, 1957) and is detailed more thoroughly in Poulos and Davis (1974). Finite depth layers were accounted for through correction factors.

### 3 IDEALISED SOIL MODEL GEOMETRY AND LOADING CONDITION

The model used for equation development assumed standard embankment geometry of a trapezoid with crest width,  $a$ , base width,  $B$ , and height,  $h$ . Its shape was assumed symmetrical around the centreline, and no lateral movement or force assumed to cross the centreline. Furthermore, the embankment was assumed rigid enough such that no stability failure occurs during simulation.

The depth of foundation modelled was placed at ten times the height of the embankment. This boundary was considered to be rigid, and was fixed in the  $y$ -direction. The far lateral boundary of the finite difference mesh were placed a distance of four times the half base width from the embankment centreline, and both limits fixed in the  $x$ -direction. By assigning the lateral and vertical dimensions in this manner, boundary effects were able to be minimised. The ground surface boundary was assumed free moving.

Surcharge loading was assumed to be instantaneous for all models, and applied following the development of in-situ conditions phase of the model. Loadings were described using an elastic model.

### 4 INPUT PARAMETERS

In modelling the lateral deformations, the input parameters of the soil properties included the bulk ( $K$ ) and shear ( $G$ ) moduli of the foundation soils, as well as the soil density,  $\rho$  of both the embankment and foundation soils. Bulk and shear moduli were calculated internally through programming a *FISH* code into the *FLAC* model, and specifying the Young's Modulus,  $E$ , and Poisson's ratio,  $\nu$ , for the model. *FISH* is the internal programming language of *FLAC* which allows user definition of variables, and in some cases, constitutive models.

Input parameters for the geometry of the embankment and foundation soils were the height of the embankment ( $h$ ), height of the clay layer ( $H$ ), and measures of the base and crest of the embankment. Due to the half symmetry assumed, these measures of base and crest width were equal to half the actual value, that is  $\frac{1}{2} B$  and  $\frac{1}{2} a$ . In order to interpret the deformation analysis, the input parameters of  $a$  and  $h$  have been normalized with  $B$ . Of the infinite possibilities, a select range of ratios for  $\nu$ ,  $h/B$ ,  $a/B$  and  $B$  were simulated in *FLAC*. The results obtained are believed to be sufficient to represent the whole range of results due to the linearity of elastic solution.

From these investigations, it was also found that the maximum lateral displacement does not necessarily occur underneath the toe of the embankment. Therefore, a correction factor was also formulated to account for how far the point under consideration was away from the toe of the embankment. This distance from the embankment toe is described within this paper using the symbol  $L_x$ .

### 5 APPROXIMATE SOLUTIONS OF LATERAL DISPLACEMENTS

#### 5.1 General

The general profile of simulated lateral soil deformations both beneath the toe and immediately adjacent to the embankment is shown in Figure 1. A triangular distribution profile similar to that used by Schmertmann et. al. (1978) to describe strain influence factors, was employed as an analytical tool to approximate the lateral displacement profile. This triangular distribution was specified by four parameters - maximum lateral displacement,  $\delta_{lat,max}$ ; depth of maximum lateral displacement,  $z_{max}$ ; influence depth,  $z_{inf}$ ; and distance from the embankment toe,  $L_x$ .

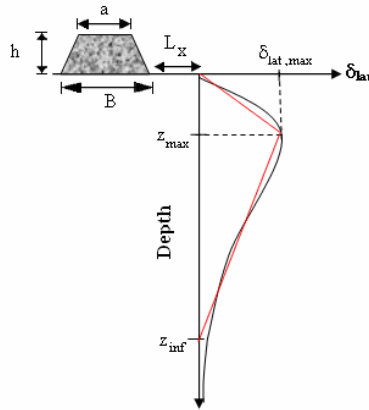


Figure 1: Sketch showing the approximated distribution profile for simulated lateral displacements

Two idealized straight lines were used to represent the curve. The first of these lines connects the point at which the lateral displacement is to be calculated for ( $L_x$ ) to the maximum lateral displacement,  $\delta_{lat,max}$ , at a depth of  $z_{max}$ . The second line is then drawn to connect this point of maximum displacement to the point where displacement is negligible and zero displacement can be assumed. The commencement point of the lateral displacement plot varied from negative to positive of the vertical axis depending on the Poisson's ratio selected, indicating that in some cases, an inward movement of soil could be expected. This phenomenon has also been observed in the field. However, study of this point was not undertaken during this analysis.

In order to non-dimensionalise the 4 parameters described above, each of the geometrical parameters -  $z_{lat,max}$ ,  $z_{inf}$ ,  $L_x$  - were divided by  $B$ , and the generalised deformation equation rearranged to describe the influence factor,  $I_{peak}$  (see Equation 2), instead of  $\delta$ . The applied pressure is denoted by  $q$  in this equation. By generalising the solutions in this manner, they can be used to suit different types of soil properties and embankment geometries.

$$I_{peak} = \delta_{lat,max} E / qB \quad (2)$$

Equations for  $I_{peak}$ ,  $z_{max}/B$ ,  $z_{inf}/B$  were initially derived for clay layers of infinite depth. Infinite depth in these situations was defined to encompass any situations in which the compressible clay layer exceeded the influence depth,  $z_{inf}$ . The factors,  $\Phi_1$  and  $\Phi_2$ , were derived for use in conjunction with  $I_{peak}$ , and are used to account for the distance ( $L_x$ ) away from the embankment toe, and also the depth of foundation layer respectively. The third factor,  $\Phi_3$ , is used in calculating the depth of maximum displacement,  $z_{max}$ , and accounts for the depth of foundation layer.

Details of the derivation of equations are discussed subsequently in Sections 5.2, 5.3 and 5.4. In order to clearly define when the infinite depth solution should be used, and when finite layer correction factors should be applied,  $z_{inf}$  is discussed first. Following  $z_{inf}$ , analysis of both  $I_{peak}$  and  $z_{max}$  are given.

## 5.2 Governing Parameters of $z_{inf}/B$

A number of steps were taken in determining the influence depth ratio,  $z_{inf}/B$ , due to embankment loading. Foremost to these, was to plot the lateral deformation profile induced in each embankment loading. Lateral displacement profiles were plotted not only at the toe of the embankment, but also at distances of 0.5B, 0.75B, B, 1.5B, 2B and 2.5B away.

Investigations showed that  $z_{inf}/B$  remained constant for the entire range of  $a/B$  and  $h/B$  tested and that of those studied, Poisson's ratio is the only governing parameter for determining influence depth. The relationship between  $z_{inf}/B$  and  $\nu$  can be expressed using Equation 3. It is evident from this equation, that with increased Poisson's ratio, the influence depth for a soil will decrease.

$$z_{inf}/B = 3.2 - 1.4\nu \quad (3)$$

### 5.3 Governing Parameters of $I_{peak}$

A study of the simulation results revealed that there was a definite connection between the magnitude of  $I_{peak}$  and the factors of Poisson's ratio,  $\nu$  and crest to base width ratio,  $a/B$ , of the embankment. Increases for both of these parameters yielded a definite increase in the value of  $I_{peak}$  (see Figure 2).

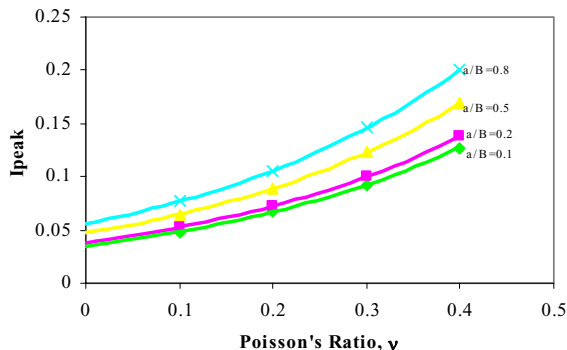


Figure 2: Plots of  $I_{peak}$  against Poisson's Ratio,  $\nu$ , for Various  $a/B$  Ratios at the Toe of an Embankment

In the context of a compressible clay layer of infinite depth (i.e.  $H > z_{inf}$ ), Equation 4 may be used to determine the peak influence factor attributable to embankment loading. The factor  $\Phi_1$ , described using Equation 5, accounts for circumstances in which the lateral deformation profile is required for points which exist away from the embankment toe.

$$I_{peak} = \left[ 0.030 \left( \frac{a}{B} \right) + 0.032 \right]^{\Phi_1, \nu} \quad (4)$$

$$\Phi_1 = 0.067 \left( \frac{L_x}{B} \right)^2 - 0.475 \left( \frac{L_x}{B} \right) + 3.25 \quad (5)$$

For depths of clay which do not exceed the influence depth,  $z_{inf}$ , and are thus considered finite, a further factor,  $\Phi_2$ , has been produced to account for the amplification of lateral deformations (see Equation 6).

$$\Phi_2 = 0.88(H/5B)^{-0.44} \quad (6)$$

This correction factor is applied following the calculation of maximum lateral displacement using  $I_{peak}$  for foundations of infinite depth. Thus, the overall maximum lateral displacement is calculated using Equation 7.  $\Phi_2$  is assumed as 1 in situations of "infinite" clay depth.

$$\delta_{lat, max} = \Phi_2 \frac{qBI_{peak}}{E_{foundation}} \quad (7)$$

### 5.4 Governing Parameters of $z_{max}/B$

As with  $z_{inf}$ , analysis suggests Poisson's ratio ( $\nu$ ) to be the only governing parameter for determination of the value of  $z_{max}/B$ , and that the position of maximum lateral displacement is irrespective of embankment geometry. The relationship between  $z_{max}$ , and  $\nu$  may be expressed through the following numerical equation:

$$z_{max}/B = 0.68\nu - 0.545 \quad (8)$$

Analysis showed that although the clay layer depth,  $H$ , had negligible difference on the position of maximum lateral displacement, the distance of the profile away from the toe did influence the result. This effect can be quantified by applying the factor outlined in Equation 9.

$$\Phi_3 = 0.056(L_x/B) + 1.0 \quad (9)$$

By combining equations 8 and 9, the overall equation for  $z_{\max}/B$  is:

$$\frac{z_{\max}}{B} = \Phi_3(0.68\nu - 0.545) \quad (10)$$

## 6 VALIDATION OF APPROXIMATE SOLUTIONS

The approximate solutions developed and derived within this paper are only applicable to short-term settlements, and thus, correspond to the lateral displacement induced as a result of the immediate vertical settlement of the foundation. Differentiation between the three different phases of settlement is notoriously difficult with regards to in-field data. Thus, in order to validate these equations, results were obtained from running the numerical model previously established for the Sunshine Motorway Trial Embankment and excluding fluid flow from the model. By not allowing pore pressure dissipation, an accurate gauge of the immediate settlement, and thus, the short-term deformations was obtained.

The approximate layout assumed for the Sunshine Motorway Trial Embankment and used for validation purposes is shown in Figure 3. As shown, this geometric arrangement consists of two trapezoids in half symmetry. The primary trapezoid corresponds to the main embankment with a crest width of 17 metres, base width of 22 metres and total height of 2.85 metres. The second, shorter trapezoid corresponds to a crest width of 33 metres, base width of 35 metres, and height of 1 metre.

Two points of comparison were selected for validation. Point A is situated at the toe of the main embankment. Point B, on the other hand, is located 6.5 metres away from Point A, at the edge of the berm. Foundation depth is assumed as one single, homogeneous layer with a thickness of 16 metres.

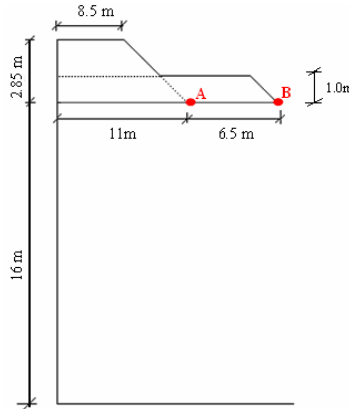


Figure 3 Approximated layout for validation of lateral displacement solutions

In accordance with the numerical model, embankment density was assumed to be  $2039 \text{ kg/m}^3$ . For Young's Modulus of the foundation, a weighted value was calculated using actual values from the layered situation. Overall, the weighted value was evaluated to 10.48 MPa. Poisson's ratio for the homogeneous foundation was also calculated using this method.

Table 1 displays a comparison of the analytical values calculated using the equations derived above with the numerical model results (assuming undrained loading). While slightly underestimating the actual magnitude, the equations produced acceptable results for points both at the toe of the embankment (Point A) and also at a short distance away from the toe (Point B). The depth at which

this maximum lateral displacement occurs was also slightly underestimated, however, with the level of underestimation being in the order of 5% or less for both profiles, this deviation is also considered acceptable. Discrepancies between the analytical and numerical modelling solutions can be primarily attributed to the approximation of a single, homogeneous layer which is used for the analytical solutions. It is acknowledged that such an approximation will be erroneous, however, is also necessary in the production of generalised equations.

Table 1 Comparison of Predicted and Actual Values for  $\delta_{lat,max}$  and  $z_{max}$

Parameter	Units	Point A		Point B	
		Predicted	FLAC	Predicted	FLAC
$\delta_{lat,max}$	mm	58.5	73.8	79.6	87.9
$z_{max}$	m	5.14	5	5.23	5
$z_{inf}$	m	28.2	n/a	28.2	n/a

In calculating the magnitude of maximum lateral displacement at Point B, both the main embankment and the berm were considered. Contributions of both the primary and secondary trapezoids were determined individually and then summed. Due to an overlap of these two trapezoids, the contributions of a third trapezoid (the overlap area) were calculated, and then subtracted from the sum of the first two. The main embankment section was considered to be the determinant embankment geometry with respect to the depth at which the maximum lateral displacement occurs, thus for this parameter, calculations were only undertaken for the primary trapezoid.

## 7 CONCLUSIONS

This paper overviewed the development of approximate analytical solutions for the lateral displacement not only beneath the toe of the embankment, but also within the adjacent soils. These analytical solutions were developed by analysing the results of FLAC simulations and include:

- A dimensionless influence factor,  $I_{peak}$ , developed from the general form of the deformation equation, and used to describe the maximum lateral deformation induced from the loading
- The normalized depth at which the maximum deformation occurs,  $z_{max}/B$
- The normalized influence depth of the deformation zone,  $z_{inf}/B$

A comparison of values obtained using these approximate solutions and results of a previously developed and verified numerical model was carried out to validate the accuracy of the solutions. It should be stressed that these solutions only approximate the short term lateral displacement induced, and does not take into account any lateral spreading due to consolidation or creep.

## REFERENCES

- Broms, B.B. 1971. "Stability of flexible structures (piles and pile groups)", *Proceedings of the 5<sup>th</sup> European Conference on Soil Mechanics and Foundations Engineering*, Vol. 2. pp 239 - 269
- Fadum, R.E. 1948. "Influence Values for Estimating Stresses in Elastic Foundations", *Proceedings of the 2<sup>nd</sup> International Conference on Soil Mechanics and Foundation Engineering*, Vol. 3, pp 77 - 84
- Huder, J. and Bucher, F. 1981. "Underpinning of a Pile Foundation in Soft Clay", *Proceedings of 10<sup>th</sup> International Conference on Soil Mechanics and Foundations Engineering*, Vol. 2. pp 741 - 745
- Osterberg, J.O. 1957. "Influence values for Vertical Stresses in Semi-Infinite Mass due to Embankment Loading", *Proceedings of the 4<sup>th</sup> International Conference on Soil Mechanics and Foundation Engineering*, Vol. 1. pp 393
- Poulos, H.G. and Davis, E.H. 1974. "Elastic Solutions for Soils and Rock Mechanics", John Wiley and Sons, New York, United States of America
- Schmertmann, J.H., Brown, P.R. and Hartman, J.P. 1978. "Improved Strain Influence Factor Diagrams", *Journal of Geotechnical Engineering Division*, Vol. 104 (8) pp 1131 - 1135